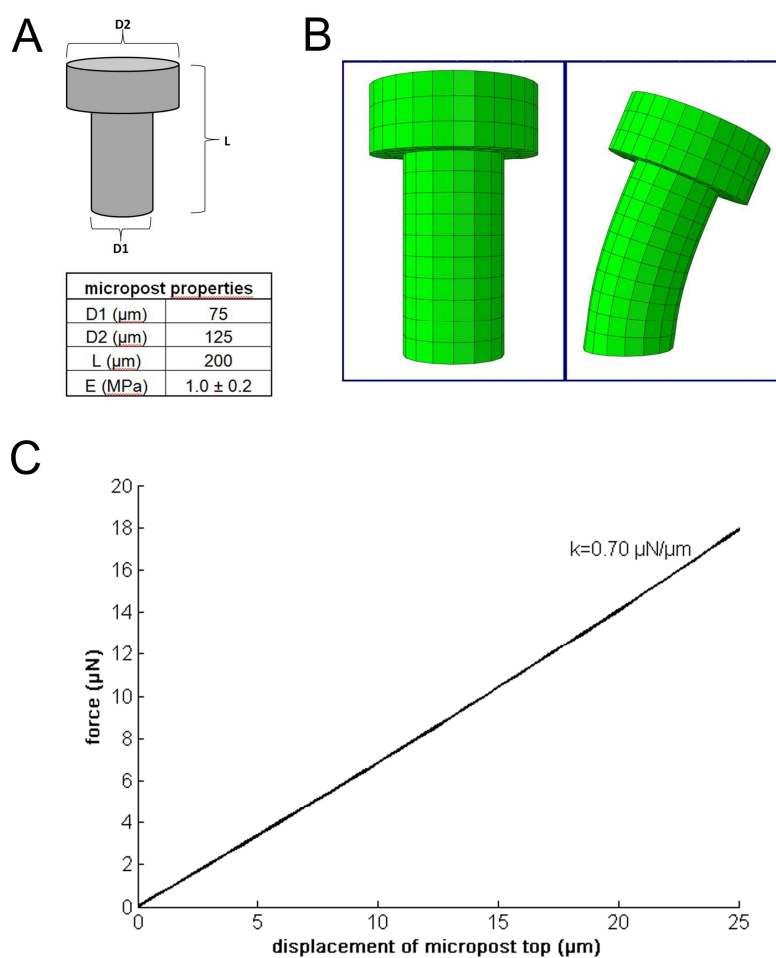
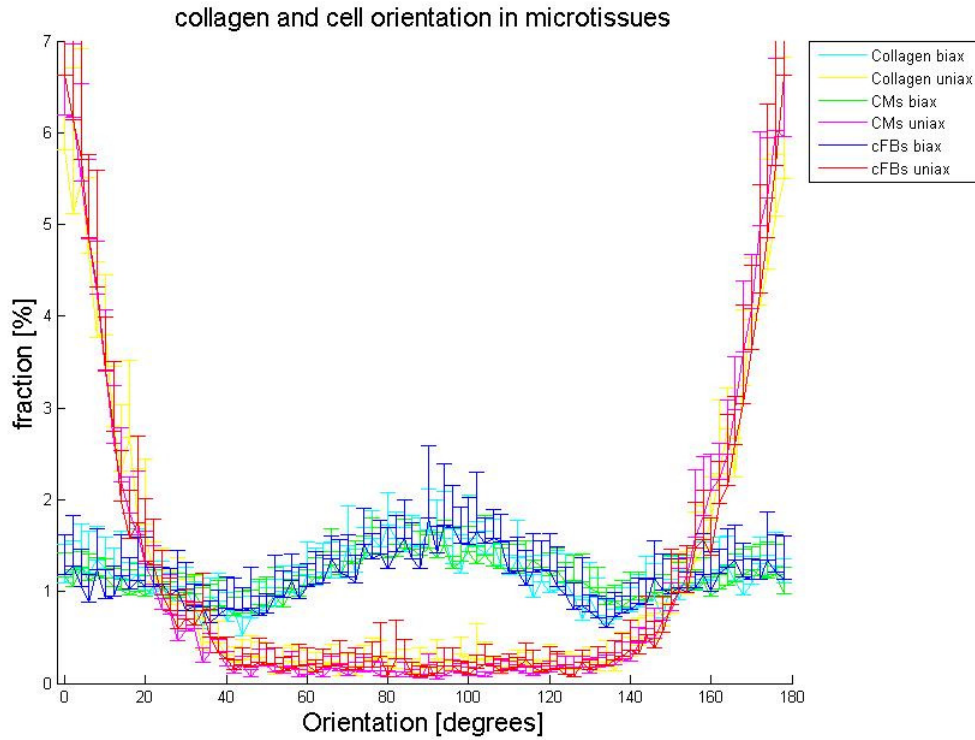


A.C.C. van Spreeuwel *et al.*

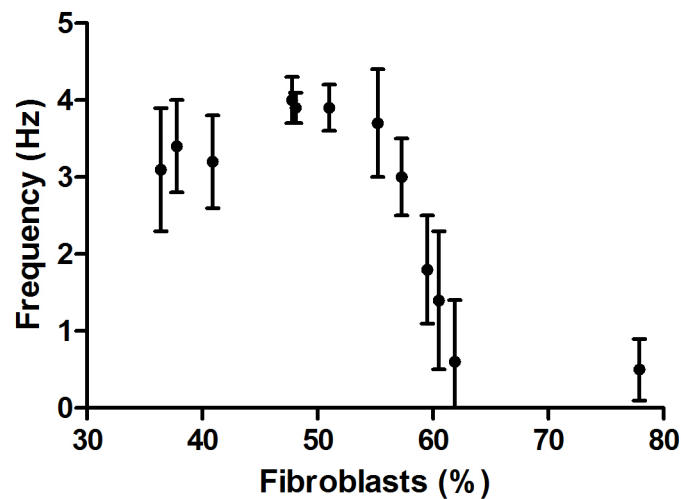
Supplementary information



Suppl. Fig. 1: Micropost bending properties. (A) Image of micropost with corresponding micropost dimensions and mean E-modulus \pm SD of the PDMS as calculated from tensile test data (N=12 from 2 batches of PDMS). (B) Finite element model of the micropost in its initial and deformed shape. (C) Plot of displacement vs. force as was calculated from the finite element model, resulting in a spring constant $k=0.70 \mu\text{N}/\mu\text{m}$.



Suppl. Fig.2: Image analysis of immunofluorescent staining showed that CMs (green and purple lines) and cFBs (blue and red lines) adopt the same orientation as the collagen fibers (turquoise and yellow lines) in both anisotropic and isotropic microtissues. Errorbars represent SD for N=10 from one representative experiment.



Suppl. Fig.3: Beating frequency versus percentage of cFBs shows that after reaching a threshold of 55% cFBs the frequency decreased rapidly. Error bars represent SD of each experimental group from two experiments with $N \geq 8$.

Video 1: Spontaneous contraction in uniaxially constrained microtissue at day two.

Video 2: Spontaneous contraction in biaxially constrained microtissue at day two.

Video 3: Spontaneous contraction in uniaxially constrained microtissue at day four.

Video 4: Spontaneous contraction in biaxially constrained microtissue at day four.

Video 5: Spontaneous contraction in uniaxially constrained microtissue at day seven.

Video 6: Spontaneous contraction in biaxially constrained microtissue at day seven.